

Probability-Density-Aware Semi-supervised Learning

Shuyang Liu, Ruiqiu Zheng¹, Yunhang Shen²,
Zhou Yu³, Ke Li, Xing Sun, Shaohui Lin
zyu@stat.ecnu.edu.cn, shenyunhang01@gmail.com

Abstract

Semi-supervised learning (SSL) assumes that neighbor points lie in the same category (*neighbor assumption*), and points in different clusters belong to various categories (*cluster assumption*). Existing methods usually rely on similarity measures to retrieve the similar neighbor points, ignoring *cluster assumption*, which may not utilize unlabeled information sufficiently and effectively. This paper first provides a systematic investigation into the significant role of probability density in SSL and lays a solid theoretical foundation for *cluster assumption*. To this end, we introduce a Probability-Density-Aware Measure (PM) to discern the similarity between neighbor points. To further improve Label Propagation, we also design a Probability-Density-Aware Measure Label Propagation (PMLP) algorithm to fully consider the *cluster assumption* in label propagation. Last, but not least, we prove that traditional pseudo-labeling could be viewed as a particular case of PMLP, which provides a comprehensive theoretical understanding of PMLP’s superior performance. Extensive experiments demonstrate that PMLP achieves outstanding performance compared with other recent methods.

Introduction

Machine Learning’s remarkable breakthroughs rely on constructing high-quality, complex labeled datasets. However, dataset annotations are increasingly costly or even infeasible in many professional areas (*e.g.*, medical and astronomical fields (Chen et al. 2020b; Xu et al. 2022)). Semi-supervised learning (SSL) has been proposed to mitigate the demand for large-scale labels by extracting information from unlabeled data with guidance from a few labeled data. The existing SSL methods are designed based on the widely accepted *assumption of consistency*, which assumes that close data points probably have the same label and data points lie in the same cluster tend to have the same labels (Zhou et al. 2003; Chapelle and Zien 2005; Iscen et al. 2019; Li et al. 2020; Zhao et al. 2022). The latter prior that points from the same category should lie in the same cluster is specifically called *cluster assumption* (Zhou et al. 2003; Iscen et al. 2019; Li et al. 2020).

In SSL, the *assumption of consistency* is usually considered by assigning the similarity between neighbor points. An enormous similarity indicates that the points tend to be in the same category. Some works use similarity to train a consistent encoder, considering that neighbor input should have neighbor features (Sohn et al. 2020). Contrastive learning learns consistent visual representations with unlabeled images (Chen et al. 2020a). Adversarial training (Miyato et al.

2018) and data augmentation (Berthelot et al. 2019; Sohn et al. 2020) are also widely applied to gain more training samples and improve the learning of representation. High-confidence pseudo-labels are propagated with close neighbor points’ predictions and labels (Isцен et al. 2019; Zhao et al. 2022; Elezi et al. 2018). Combining consistent encoder and pseudo-labeling significantly improves the model performance (Isцен et al. 2019). Recently, the widely-used SSL framework often consists of supervised loss to take full consideration of labeled data, unsupervised loss to improve the quality of pseudo labels, and consistency loss to encourage a consistent encoder (Zhao et al. 2022; Berthelot et al. 2019; Zheng et al. 2022).

However, these works fail to fully consider *assumption of consistency*, for they do not use the prior of *cluster assumption*. When calculating the similarity between points, their measurements seldom consider the cluster prior. Considering that the points close to the decision boundary may be closer to points from other categories than some points in the same categories, these algorithms may be misled by wrongly assigning neighbors’ labels. Our proposed solution, the Probability-Density-Aware Measurement (PM), has the potential to fully utilize the *cluster assumption* through the incorporation of density information and could address the limitations of existing algorithms. A natural thought goes that for two points with different clusters, their path tends to traverse low-density regions. We statistically prove the thought and demonstrate that the path probably goes through low-density areas. The theorem indicates that density information significantly helps to consider the *cluster assumption* and serves as the keystone of PM.

With PM, we can better measure the similarity between points. We deploy PM into Label Propagation to select better neighbors and generate higher-confidence pseudo-labels. The new algorithm is named Probability-Density-Aware Label-Propagation (PMLP). To show PM’s superiority and generality, we prove that traditional pseudo-labeling is a particular case of PMLP, which indicates that PMLP should always be better with just minor optimization. PM can be easily implemented to complement many popular SSL methods involving label propagation (Zhou et al. 2003; Iscen et al. 2019; Zhao et al. 2022; Elezi et al. 2018); we deploy PM to the best performance LPA algorithm (Zhao et al. 2022) to implement the experiment. Through comprehensive experiments on benchmark datasets, we show that PMLP achieves noticeable performance improvement compared to some of the most powerful approaches. In general, our contribution can be summarized into three points:

- We first propose a theoretical description to *cluster assumption*, which reveals that probability density can help make full use of SSL’s prior;
- We introduce a new Probability-Density-Aware similarity measurement (PM) to fully consider SSL’s cluster prior. Probability-Density-Aware Label-Propagation (PMLP) is proposed based on PM. We mathematically prove PMLP’s superiority and generality;
- Extensive experiments are conducted to validate the effectiveness of PMLP. For example, on CIFAR100 with

¹Equally contribution with the first author.

²The corresponding author, Tencent Youtu Laboratory.

³The corresponding author, East China Normal University.

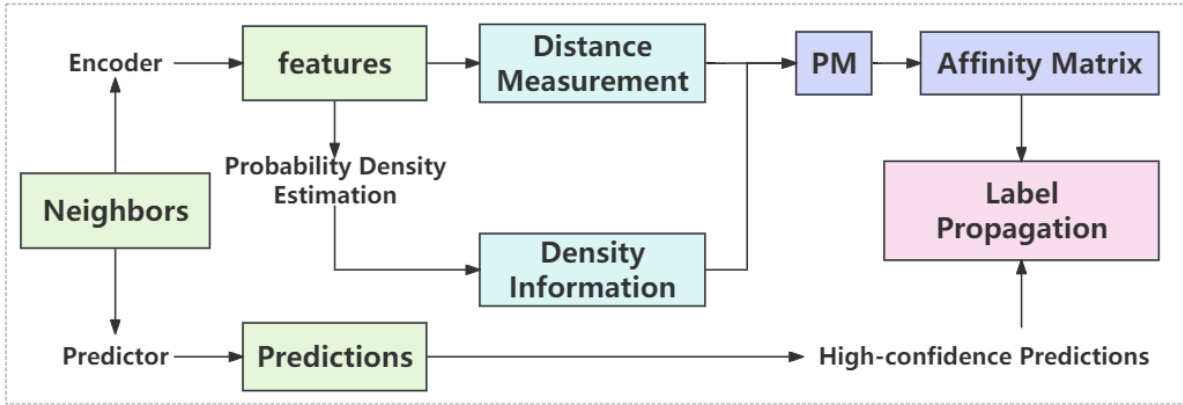


Figure 1: The procedure of PMLP. First, we select the neighbor points and extract their features. Then, we calculate the densities on the path; the density information is used to construct the Probability-density-aware Measure(PM). PM can fully consider the *cluster assumption*. Finally, high-confidence predictions are used for pseudo-labeling with an affinity matrix.

400 labeled samples, we can surpass the baseline model by 3.52% and surpass the second-best algorithm by 1.21%.

Related Works

Consistency Regularization

The *assumption of consistency* is widely accepted in SSL. Its foundation is generating well-consistency models that exhibit similar features for similar inputs. The works in (Hinton, Osindero, and Teh 2006; Bengio et al. 2006) improved consistency via self-training and finetuning the model with labeled data. *II – model* (Laine and Aila 2016) reduces the consistency loss between images and their augmentations, or between outputs and temporal average outputs. Mean-teacher (Tarvainen and Valpola 2017) reduces consistency loss between current weights and temporal average weights. Data augmentation can help to extract more feature information (Miyato et al. 2018; Elezi et al. 2018). Recent algorithm (Chen et al. 2020b) involved contrastive learning to improve the model consistency, and LASSL (Zhao et al. 2022) generated class-aware contrastive learning by limiting the comparisons within the same class. However, these works fail to produce pseudo-labels directly.

Pseudo-labeling

Generating high-confidence pseudo-labels for unlabeled data is a widely used policy in SSL. A simple yet intuitive approach considers high-confidence probability (higher than a threshold τ) vectors to be accurate and assigns them pseudo-labels (Sohn et al. 2020). Freematch and Adsh (Wang et al. 2022; Guo and Li 2022) adaptive adjust threshold τ to improve the pseudo-label quality. Some early pseudo-labeling algorithms (Lee 2013; Sajjadi, Javanmardi, and Tasdizen 2016; Shi et al. 2018) rely heavily on predictions, while recent frameworks prefer graph-based label propagation yielding better consideration of *assumption of consistency* (Zhou et al. 2003; Iscen et al. 2019; Zhao et al.

2022; Douze et al. 2018). Graph transduction game (Elezi et al. 2018; ?) fixes the graph and lacks a weighting mechanism. Some statistical methods (Zhou et al. 2003) take a reasonable consideration of *assumption of consistency* by calculating the affinities via the first-order similarity between features and iteratively spread labels to their neighbors. The strategy can extend to the high-dimensional feature space in deep learning (Isken et al. 2019; Zhao et al. 2022). Co-match *et al.* (Li et al. 2021) introduces graphic information in contrastive learning and smooths pseudo-labels with a memory bank. However, these works fail to fully consider the *cluster assumption*.

Density-aware Methods

Although the above techniques effectively select close neighbors, the *cluster assumption* is not sufficiently considered, and they fail to distinguish neighbors' cluster affiliation directly. Some works intuitively point out that the decision boundary tends to be placed in a low-density region (Chapelle and Zien 2005; Li et al. 2020), and this prior helps consider *cluster assumption*. Wasserman *et al.* (Azizyan, Singh, and Wasserman 2013) proposes a density-sensitive distance metric that provides a lower value when the points are located in different clusters. Connectivity kernel (Chapelle and Zien 2005; Bousquet, Chapelle, and Hein 2003) can utilize the detection of density variations along a path to determine whether two points lie in the same cluster. These statistical methods can thoroughly consider *cluster assumption*, but their optimization in high-dimensional space needs expensive computation. Recently, DNA and DPLP (Li et al. 2020) prefer higher-density neighbors and construct a density-ascending path for pseudo-labeling. However, their density is cosine similarity, which harms the theoretical guarantee and statistical interpretability. Simmatch (Zheng et al. 2022) tries to optimize pseudo labels with marginal distribution, but labeled data in SSL is few.

Our algorithm aims at providing a general framework to fully consider the *cluster assumption* by density-aware distance, and thus produce high-quality pseudo-labels.

Methodology

A Statistical Explanation To *Cluster Assumption*

It has been widely accepted that with *cluster assumption*, points in the same cluster tend to lie in the same category. In the previous work, however, it still lacks mathematical investigation. This section presents an innovative statistical explanation demonstrating probability density is crucial in leveraging the *cluster assumption*. To lay a theoretical analysis, without loss of generality, we assume the points in the feature space are widely accepted sub-gaussian random vectors. Then we have the **Theorem1**:

Theorem1 Suppose two sub-gaussian random vectors X_1, X_2 with mean μ_1, μ_2 . Denote x_1, x_2 randomly sampled from X_1, X_2 , and $\gamma(x_1, x_2)$ (Azizyan, Singh, and Wasserman 2013) is a continuous finite path from x_1 to x_2 . For any $\tau \in R$, denote $p(x)$ is the probability density of point x estimated by Kernel Density Estimator (KDE), define event:

$$C_\tau : \{\exists x \in \gamma(x_1, x_2), p(x) \leq \tau\}.$$

Then with $\|\mu_1 - \mu_2\|_2^2 \rightarrow \infty$, we have:

$$P(C_\tau) \rightarrow 1.$$

We can further prove that for two sufficiently dispersed X_1, X_2 , almost every point on the straight line between x_1, x_2 traverses a low-density region.

Corollary1 Specifically take $\gamma(x_1, x_2)$ in **Theorem1** as a straight line and $x \in \gamma(x_1, x_2)$ distributes uniformly. For $\forall \tau \in R$, with sufficient large $\|\mu_1 - \mu_2\|_2^2$, we have:

$$\lim_{\|\mu_1 - \mu_2\|_2^2 \rightarrow \infty} P(\{x : p(x) \leq \tau, x \in \gamma(x_1, x_2)\}) \rightarrow 1.$$

We have statistically proved that density information helps consider the *cluster assumption* besides traditional distance measures. Specifically, their path probably traverses a low-density region when the points lie in different clusters. We simply choose $\gamma(x_1, x_2)$ as the connecting line $l(x_1, x_2)$ to save computation and equidistant select K samples $\{x_{i,j}^1, \dots, x_{i,j}^k\}$ along $l(x_1, x_2)$. We estimate their densities $\{p(x_{i,j}^1), \dots, p(x_{i,j}^k)\}$ with Kernel Density Estimator(KDE) and the generated density information is denoted as $\{I(p_{i,j}) | \{p(x_{i,j}^1), \dots, p(x_{i,j}^k)\}\}$. We hope $I(p_{i,j})$ tends large when $l(x_i, x_j)$ traverses inside one cluster and tends small when $l(x_i, x_j)$ traverses among different clusters.

With any traditional distance measure $D(x_i, x_j)$ (such as first-order similarity, Euclidean distance, and cosine similarity), we propose our density-aware distance measure:

$$\begin{cases} d(x_i, x_j) = I(p_{i,j})D^{-1}(x_i, x_j), & \text{if } i \neq j; \\ d(x_i, x_j) = 0, & \text{if } i = j. \end{cases}$$

We name $d(x_i, x_j)$ as Probability-Density-Aware Measure(PM). The **Theorem2** presents four choices of $I(p_{i,j})$ and proves PM's superiority. In PM, the distance measure

$D(x_i, x_j)$ reflects the *neighbor assumption* that neighbor points tend to have the same label, and the density information $I(p_{i,j})$ reflects the *cluster assumption* that features lie in different clusters tend to have different labels, thus takes full consideration of *assumption of consistency*.

Probability-Density-Aware Measure Label-Propagation

Traditional Label Propagation Algorithm (LPA) (Zhou et al. 2003; Iscen et al. 2019; Zhao et al. 2022) search neighbor points by a distance measure $D(x_i, x_j)$ including first-order similarity, cosine similarity, and Euclidean distance, which lack consideration of *cluster assumption*. We propose Probability-Density-Aware Measure Label-Propagation (PMLP) by introducing the PM $d(x_i, x_j) = I(p_{i,j})D^{-1}(x_i, x_j)$ into pseudo-labeling. Theorem 2 lays a theoretical foundation for the good performance of PMLP.

Suppose we have observations O and labeled data (X^L, Y^L) , unlabeled data and its prediction $(X^U, p(X^U))$. As assumed in LPA, we propagate high-confidence predictions to low-confidence predictions by similarity measures between neighbor points.

As a familiar setting in LPA, we use KNN to choose K nearest neighbors in feature space O , and then we get new $O^{LP} = \{o_1^{LP}, \dots, o_K^{LP}\}$, and the corresponding $Y^{LP} = \{y_1^{LP}, \dots, y_K^{LP}\} \in \{p(X^U)\} \cup \{Y^L\}$. Then we reweight Y^{LP} by threshold τ :

$$\begin{aligned} y_t^{LP, \text{high}} &= I(\max(y_t^{LP}) \geq \tau) y_t^{LP}, \\ y_t^{LP, \text{low}} &= I(\max(y_t^{LP}) < \tau) y_t^{LP}, \end{aligned} \quad (1)$$

where $Y^{LP, \text{high}}$ includes high-confidence predictions $y_t^{LP, \text{high}}$ and ground-truth labels Y^L . Denote any distance measurements between features as $D(o_i^{LP}, o_j^{LP})$ in traditional LPA. To fully consider *cluster assumption*, we introduce PM $d(x_i, x_j)$ to introduce the density information between two features o_i^{LP}, o_j^{LP} . Then we get the reweighted adjacent matrix W' :

$$W'_{i,j} = \begin{cases} 0, & \text{if } i = j, \\ I(p_{i,j})D^{-1}(o_i^{LP}, o_j^{LP}), & \text{if } i \neq j, \end{cases} \quad (2)$$

Then, the pseudo-labels are generated by iteratively propagating the high-confidence predictions to their close and same-cluster neighbors based on the affinity matrix W' . Denote $\hat{Y}'^{LP}(i)$ implies the propagated pseudo-label in i -th iteration. Note D the diagonal matrix with (i, i) -th equal to the sum of the i -th row of W' , and iteratively propagate the label information to unlabeled points:

$$\hat{Y}'^{LP}(i) = \alpha D^{-\frac{1}{2}} W' D^{-\frac{1}{2}} \hat{Y}'^{LP}(i-1) + (1-\alpha) Y^{LP, \text{high}}. \quad (3)$$

We get the final optimal form \hat{Y}'^{LP} :

$$\hat{Y}'^{LP} = (I - \alpha D'^{-\frac{1}{2}} W' D'^{-\frac{1}{2}})^{-1} Y^{LP, \text{high}}.$$

And the final pseudo-label \hat{Y}^{*LP} is combined by \hat{Y}'^{LP} and our prediction $Y^{LP, \text{low}}$:

$$\hat{Y}^{*LP} = \eta \hat{Y}'^{LP} + (1-\eta)(Y^{LP, \text{low}}). \quad (4)$$

Algorithm 1: The algorithm for density-aware label propagation

Input:

K, Y^{LP}, O^{LP} , threshold τ, k, n, α, η .

Output: density-aware pseudo-label \hat{Y}^{*LP}

- 1: Choose K nearest neighbor points in features O^{LP} ;
 - 2: Separate $Y^{LP,high}$ and $Y^{LP,low}$ by Eq. 1 with τ ;
 - 3: For points in $Y^{LP,low}$ and $Y^{LP,high}$, calculate the distance $D(x_i, x_j)$.
 - 4: Get k -equal division points on the connecting line, for each point in $o_{i,j}^1, \dots, o_{i,j}^k$, select n neighbors to calculate density $p_{i,j}$ with KDE;
 - 5: Reweight W with $I(p_{i,j})$ as Eq. 2, get W' ;
 - 6: Propagating the label with W', α by Eq. 3, get Y'^{LP} ;
 - 7: Mix the propagated label Y'^{LP} and Y^{LP} by Eq. 4 with η , get final density-aware pseudo-label \hat{Y}^{*LP} .
-

The superiority and generalization of PMLP lie in its good theoretical guarantee: whatever the choice of $D(o_i^{LP}, o_j^{LP})$ and loss function $L(Y^P, \hat{Y}^{*LP})$, we prove that, when $I(p_{i,j})$ is chosen as:

$$\begin{cases} I(p_{i,j}) = \max\{p_t(i,j), t = 1, 2, \dots, k\}, & \text{if } i = j, \\ I(p_{i,j}) = \min\{p_t(i,j), t = 1, 2, \dots, k\}, & \text{if } i \neq j, \\ I(p_{i,j}) = \text{avg}(\{p_t(i,j), t = 1, 2, \dots, k\}), & \text{if } i \neq j, \\ I(p_{i,j}) = Q_t(\{p_t(i,j), t = 1, 2, \dots, k\}), & \text{if } i \neq j, \end{cases}$$

where $\text{avg}(\cdot)$ denotes the mean and $Q_t(\cdot)$ denotes the t -quantile, in our implementation, we take it as the median. The procedure of PMLP is in pseudo code 1.

We prove that PMLP can consistently outperform traditional LPA. Traditional LPA is a particular case of PMLP, indicating both PMLP's superiority and reasonableness.

Theorem 2. *Denote the model parameter in one iteration as θ . And let \mathcal{L}_U be the unsupervised loss between predictions and pseudo-labels. Denote Y^P as the set of predictions, \hat{Y}^{*LP} and \hat{Y}^{LP} be the pseudo-labels generated by PMLP and traditional LPA with any $D(\cdot, \cdot)$ (Zhou et al. 2003; Iscen et al. 2019; Zhao et al. 2022). Suppose we calculate the probability density by KDE with exponential kernel and bandwidth h . Then \mathcal{L}_U satisfies:*

$$\min_{\theta \in \Theta, h \in R} \mathcal{L}_U(Y^P, \hat{Y}^{*LP}) \leq \min_{\theta \in \Theta} \mathcal{L}_U(Y^P, \hat{Y}^{LP}).$$

The Competitive Pseudo-Labeling

Recent pseudo-labeling algorithms combine a consistent encoder, considering that a better encoder can generate better representations and facilitate the pseudo-labeling (Isцен et al. 2019; Zhao et al. 2022; Berthelot et al. 2019; Sohn et al. 2020; Zheng et al. 2022). We inherit this framework in the implementation of PMLP. We choose the Label-guided Self-training approach to Semi-supervised Learning (LASSL) (Zhao et al. 2022) as our baseline. As the best-performing label-propagation algorithm in recent years,

LASSL still behaves dissatisfiedly compared with other recent algorithms. We hope deploying PMLP with the LASSL framework will allow it to surpass recent algorithms, thus demonstrating the full potential of label propagation under *cluster assumption*.

In our implementation, we update the model with three losses: the supervised cross-entropy loss \mathcal{L}_S , the class-aware contrastive (CACL) loss \mathcal{L}_C (Zhao et al. 2022), and the unsupervised cross-entropy loss \mathcal{L}_U .

Denote θ as the model's parameters, labeled dataset $X^L = \{X_L, Y_L\}$, the model takes a consideration of labeled data by minimizing \mathcal{L}_S :

$$\mathcal{L}_S(X^L; Y^L; \theta) := CE(X^L; Y^L; \theta).$$

Denote the weak and strong augmentation of input x as $a(x), A(x)$, denote $z_i^L = G(a(x_i))$ and $z_j^U = G(A(u_j))$ as the output features for both labeled and unlabeled data. In the t -th iteration, note $Y_{t-1} = \{y_1^L, \dots, y_B^L\} \cup \{y_1^U, \dots, y_{\mu_B}^U\}$ all predictions of labeled and unlabeled data, for $y_i, y_j \in Y_{t-1}$, introduce the instance relationships to help the contrastive learning:

$$w_{i,j} = \begin{cases} 1, & \text{if } i = j, \\ 0, & \text{if } i \neq j \text{ and } y_i \cdot y_j \leq \epsilon, \\ y_i \cdot y_j, & \text{if } i \neq j \text{ and } y_i \cdot y_j \geq \epsilon, \end{cases}$$

where ϵ is a hyper-parameter determining the confidence that two instances belong to the same category.

Then we get \mathcal{L}_C to help learning a good representation:

$$\mathcal{L}_C = -\sum_{i=1}^{|Y_{t-1}|} \log\left(\frac{\sum_{j=1}^{|Y_{t-1}|} w_{i,j} \exp(\frac{z_i \cdot z_j}{T})}{\sum_{j=1, j \neq i}^{|Y_{t-1}|} \exp(\frac{z_i \cdot z_j}{T})}\right),$$

where T is temperature hyper-parameter (Chen et al. 2020b).

Denote $Y^U = \{y_1^U, \dots, y_{\mu_B}^U\}$ the predictions of unlabeled data Unsupervised loss \mathcal{L}_U encourages predictions to be consistent with PMLP's confidence pseudo-labels Y^{*LP} , which in turn encourages consistency encoder and helps to improve the pseudo-labeling:

$$\mathcal{L}_U = I(y_j^U \geq \tau)H(Y^U, \hat{Y}^{*LP}).$$

Combine the three losses, we aim to update the model's parameter θ to minimize the loss function \mathcal{L} :

$$\min_{\theta \in \Theta} \mathcal{L} = \min_{\theta \in \Theta} (\mathcal{L}_S + \mathcal{L}_U + \mathcal{L}_C).$$

Experiments

Experiment Setup

⁴ We present comprehensive experiments of PMLP across extensive datasets, including SVHN (Krizhevsky and Hinton 2009), CIFAR10 (Krizhevsky and Hinton 2009), and CIFAR100 (Netzer et al. 2011), STL-10 (Adam Coates 2011). Following the standard protocol of SSL (Zhao et al. 2022; Zheng et al. 2022; Wang et al. 2022; Chen et al. 2023; Yang et al. 2023), we randomly select 40 and 250 labeled samples

⁴Code: <https://github.com/sdagfgaf/Probability-Density-aware-Semi-supervised-Learning>

Method	CIFAR10		CIFAR100		SVHN		STL-10	
	40 labels	250 labels	400 labels	2500 labels	40 labels	250 labels	40 labels	1000 labels
Pseudo-label (2013)	25.39±0.26	53.51±2.20	12.55±0.85	42.26±0.28	25.39±5.6	79.79±1.09	25.31±0.99	67.36±0.71
Mean-Teacher (2017)	29.91±1.60	62.54±3.30	18.89±1.44	54.83±1.06	33.81±3.98	96.43±0.11	29.28±1.45	66.10±1.37
MixMatch (2019)	63.81±6.48	86.37±0.59	32.41±0.66	60.24±0.48	69.40±3.39	96.02±0.23	45.07±0.96	88.3±0.68
UDA (2019)	89.33±3.75	94.84±0.06	53.61±1.59	72.27±0.21	94.88±4.27	98.01±0.02	62.58±3.44	93.36±0.17
ReMixMatch (2019)	90.12±1.03	93.70±0.05	57.25±1.05	73.97±0.35	79.96±3.13	97.08±0.48	67.88±6.24	93.26±0.14
FixMatch (2020)	92.53±0.28	95.14±0.05	53.58±0.82	71.97±0.16	96.19±1.18	98.03±0.01	64.03±4.14	93.75±0.33
ReFixMatch (2023)	95.06±0.01	95.17±0.05	53.88±1.07	72.72±0.22	71.40±4.21	94.26±0.3	97.85±1.23	98.11±0.03
Softmatch (2023)	94.89±0.14	95.04±0.09	62.40±0.24	73.61±0.38	97.54±0.24	97.99±0.01	77.78±3.82	94.21±0.15
EPASS (2023)	94.69±0.1	94.92±0.05	61.12±0.24	74.32±0.33	97.02±0.02	97.96±0.02	84.39±2.48	94.06±1.42
Freematch (2023)	95.1±0.04	95.12±0.18	62.02±0.42	73.53±0.2	98.03±0.02	98.03±0.01	84.46±0.55	94.37±0.15
Shrinkmatch (2023)	94.92	95.26	64.64	74.83	97.49	98.04	85.98	94.18
LASSL (2022,baseline)	95.07±0.78	95.71±0.46	62.33±2.69	74.67±0.65	96.91±0.52	97.85±0.13	81.57±0.36	94.23±0.26
PMLP+LASSL (Ours)	95.42±0.32	95.76±0.14	65.85±0.8	75.27±0.19	97.85±0.31	98.10±0.05	85.53±1.92	94.53±0.53
Outperform than LASSL	+0.35	+0.05	+3.52	+0.60	+0.94	+0.25	+3.96	+0.30

Table 1: Performance comparison on CIFAR10, CIFAR100, SVHN, and STL-10. We show the mean accuracy from 5 experiments and the standard deviation.

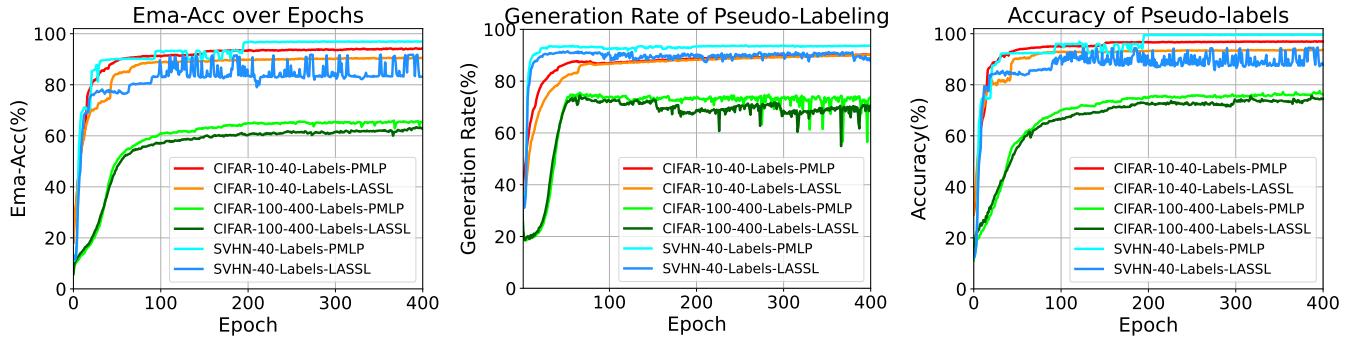


Figure 2: Left: ema-accuracy of models. Middle: rate of high-quality pseudo-labels. Right: rate of correct high-quality labels.

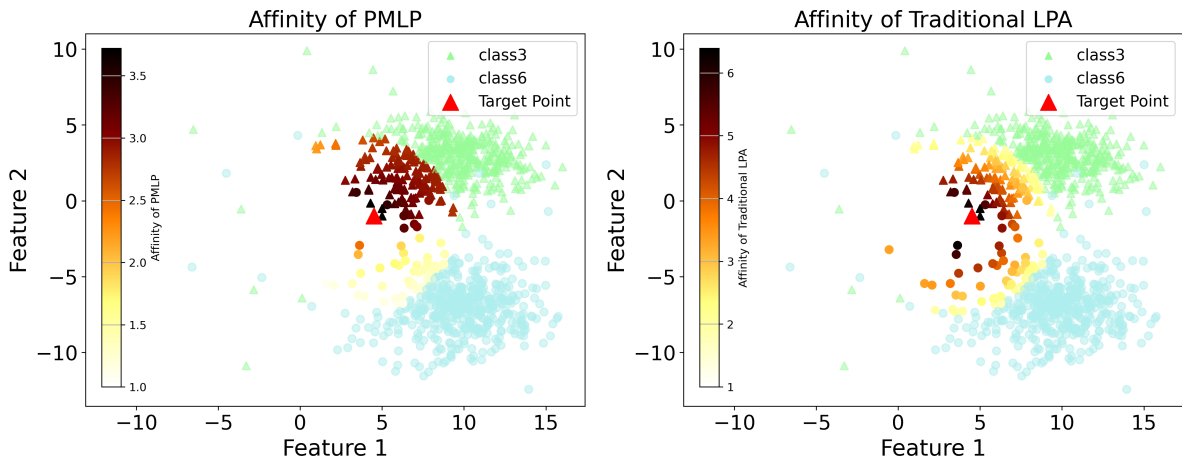


Figure 3: Different colors represent different distances between the target point and neighbor points. Black represents a close distance and a higher affinity. The left one chooses PM as the distance measure, and the right one chooses traditional first-order similarity. PMLP tends to choose neighbors within one cluster, and LPA equally chooses neighbors with different clusters.

Epoch	0-4	5-9	10-14	15-19
Time(s), PMLP	748.4	747.3	747.1	747.0
Time(s), KDE	3733.0	4244.0	4166.6	4189.0

Table 2: Running time for using KDE and our PMLP to compute the density.

from SVHN and CIFAR10. For CIFAR100, 400 and 2,500 labeled samples are randomly selected. For STL-10, we select 40, 1000 labeled samples.

For SVHN and CIFAR10, we use WideResNet-28-2 as the encoder to generate representations. For CIFAR100, encoder is WideResNet-28-8. For STL-10, encoder WideResNet-37-2. The predictor is a one-linear layer network. In the CACL, we calculate z_i with a 2-layer MLP projector. The batch size includes 64 unlabeled and 448 labeled points. In the label-propagation process, we select $1.5 \times N$ nearest neighbors, where N represents the dataset category. In PMLP, we use $\alpha = 0.8$, $\eta = 0.2$, and $\tau = 0.95$. In CACL, ϵ is set to 0.7. Optimization is performed using the SGD optimizer with a momentum of 0.9 and a weight decay of 5×10^{-4} . The learning rate follows a cosine decay schedule. For KDE, we chose a bandwidth of $h = 5$ for SVHN, CIFAR10, and CIFAR100, and $h = 3$ for STL-10. In KDE, we select 512 points for CIFAR10 and SVHN, and the nearest 45 points for CIFAR100 and STL-10.

Results On SVHN, CIFAR10, CIFAR100, STL-10

Tab. 1 compares the average testing accuracy of PMLP over 5 runs against both classical algorithms and recent SOTA SSL approaches (Zheng et al. 2022; Wang et al. 2022; Chen et al. 2023; Yang et al. 2023; Nguyen 2024; Zhao et al. 2022; Nguyen 2023). Here we set $I(p_{i,j}) = \text{avg}(\{p_t(i,j), t = 1, 2, \dots, k\})$, $K = 1$. PMLP consistently outperforms other SOTA approaches on CIFAR10 and CIFAR100 under all settings. With 400 labeled samples in CIFAR100, PMLP achieves an accuracy of 65.85%, surpassing the second-best ShrinkMatch (Yang et al. 2023) by 1.21% and improving our baseline LASSL with 3.52%. We also improved our baseline LASSL with 0.6% thus surpassing the second-best ShrinkMatch with 0.44%. On CIFAR10, PMLP always surpasses ShrinkMatch by more than 0.5%. With 40 labeled samples in STL-10, PMLP reaches an accuracy of 85.53%, improving our baseline model LASSL with 3.96%; for SVHN with 40 labels, our PMLP can outperform the baseline LASSL with 0.94%, while still competitive compared with the SOTA.

PMLP Generates Better Pseudo-labels

In this section, we design experiments to show that PMLP generates better pseudo-labels. Fig. 2 shows that LASSL and PMLP generate almost the same number of high-confidence pseudo-labels, but PMLP’s pseudo-labels are more accurate. It directly explains PMLP’s superior performance while implying that traditional LPA brings more misleading wrong labels into training, harming the model’s performance.

We also visually show the PMLP’s selected neighbors in the feature space. By *Theorem1*, with the same distance, we tend to choose neighbors in the same cluster and reject the neighbors in the different clusters. We implement PMLP and classical LPA with 40 CIFAR10 labeled samples and output 64-dimensional features. Principal component analysis (PCA) is applied, and we select the two most important principal components and plot them in Fig. 3. We select the target point from class 3 and its nearest 200 neighbors. In Fig. 3, we deploy PMLP and the classical LPA (Zhou et al. 2003; Iscen et al. 2019; Zhao et al. 2022) and color the neighbors according to the value of $d(x_i, x_j)$ and $D(x_i, x_j)$. The deeper color represents a closer distance and more significant affinity. It shows that PMLP tends to choose neighbors in the same cluster. In PMLP, we introduce density information $I(p_{i,j})$ into $d(x_i, x_j)$; some neighbors in the other clusters are chosen but assigned with a lower affinity and tend to be diminished in the LPA process.

Acceleration Results Of PMLP

We introduce the density information $I(p_{i,j})$, and the probability density is calculated with KDE. A natural thought goes that KDE is expensive to compute. Considering we choose N samples on the connecting line and pick up n support points each time for KDE, $O(N^2kn)$ computation is needed. The KDE from Sklearn runs only on the CPU, leading to slower calculations. We use the exponential kernel $K(\cdot)$ in KDE to promote the divergence and design a GPU-based KDE, which can reach $\times 5$ acceleration Tab. 2. The details can be seen in the Appendix⁵. We further compare the average time consumption in training between PMLP and our baseline LASSL in Tab. 3, indicating that PMLP does not cost too much time (less than about 5%) than traditional LPA.

Ablation Studies

The Effect Of $I(p_{i,j})$ In Tab. 5, we compare PMLP’s performance with different $I(p_{i,j})$ and different K points on the connecting line. We deploy the experiment with the CIFAR10 dataset, 40 labeled samples. We use simplify notations for $I(p_{i,j})$, such as $\text{avg}(\{p_t(i,j), t = 1, 2, \dots, k\}) = \text{avg}(p_t(i,j))$. However, it can be seen that $\max(\{p_t(i,j)\})$ and $\min(p_t(i,j))$ are unstable with K . Meanwhile, the $\text{avg}(p_t(i,j))$ and $Q_t(p_k(i,j))$ keeps a stable performance. A thought goes that $\min(p_t(i,j))$ and $\max(p_t(i,j))$ are easily affected by singular points with an outlier density: some high-confidence points may be diminished by $\min(p_t(i,j))$, and incorrect neighbors from the other cluster may be enhanced by $\max(p_t(i,j))$. The mean and median can sufficiently use the density information to get a stable result.

We point out that Tab. 4 does not conflict with our **Theorem2**, considering that we forgo sufficiently fine-tuning the bandwidth h for $\max(p_t(i,j))$, $\min(p_t(i,j))$ considering $\text{avg}(p_t(i,j))$ is more efficient and convenient options.

A Mild Density-aware Strategy Inspired by Tab. 5, a thought goes that $I(p_{i,j})$ reflects the *cluster assumption*, but it does not serve as a sufficient statistic. Thus an incorrect

⁵Appendix: <https://arxiv.org/submit/6072244/view>

Dataset	Method	Average Time (s/epoch)	Average Time Across Different Iterations (s/epoch)			
			1-256	257-512	513-768	769-1024
STL-10	LASSL	615.21	593.81	625.56	618.04	623.40
	LASSL+PMLP	648.08(+ 5.34%)	734.59(+ 23.71%)	652.42(+ 4.29%)	606.64(- 1.85%)	598.69(- 3.96%)
CIFAR10	LASSL	211.41	255.52	196.10	196.66	197.35
	LASSL+PMLP	217.94 (+ 3.09%)	260.05 (+ 1.77%)	203.72 (+ 3.89%)	203.52 (+ 3.89%)	204.46 (+ 3.60%)

Table 3: Overall average time and average time of different iterations for different methods on STL-10 and CIFAR-10 datasets.

Bandwidth	$I(p_{i,j})$	$K=1$	$K=3$	$K=5$
h=5	$\min(p_k(i,j))$	94.75	88.82	93.70
	$\max(p_k(i,j))$	95.42	95.19	87.56
	$\text{avg}(p_k(i,j))$	95.61	95.35	95.19
	$Q_t(p_k(i,j))$	94.97	95.62	95.45
$h \rightarrow +\infty$, LASSL	None	95.30		

Table 4: Comparison of different K and $I(p_{i,j})$ on CIFAR10 dataset with 40 labeled data.

Bandwidth	$h=0.01$	$h=0.5$	$h=5$	$h=100$	$h=+\infty$	LASSL
Acc	63.34	65.42	66.5	64.32	62.50	62.33
Density Ratio	1.73	1.39	1.09	1.009	1	1

Table 5: Ablation study on CIFAR100 with 400 labeled data.

prior at the beginning may severely mislead the training. It motivates us that it’s better to take PMLP as a mild punishment that does not reject the far neighbors firmly and control the PM $d(x_i, x_j)$ with a comparably slight disparity.

We choose the $I(p_{i,j}) = \text{avg}(\{p_t(i,j), t = 1, 2, \dots, k\})$ to deploy PMLP and fine-tune the bandwidth h to attenuate the influence of density information, as h significantly impacts the KDE. Tab. 4 presents the accuracy of the PMLP on CIFAR100 with different bandwidth h , $K = 1$. When h is relatively small, the density of the midpoints shows significant differentiation. Thus, the affinity matrix W' is notably influenced by the density information $I(p_{i,j})$ and efficiently diminishes the far neighbors. The densities become similar when the h is relatively large, and the W' mildly obsoletes the low-confidence neighbors. By **Theorem2**, setting $h \rightarrow \infty$ degenerates PMLP into a classical LPA (Zhou et al. 2003; Iscen et al. 2019; Zhao et al. 2022). When $h = \infty$, the accuracy of PMLP indeed converges to LASSL, which indicates that PMLP degenerates to classical LPA.

Effect of Neighbor Point Numbers N For a fair comparison with our baseline LASSL, we keep the same choice of $1.5K$ neighbors in LPA. It is still a matter of whether more or fewer neighbors will bring better performance. Then we try other choices in Tab. 6 for the ablation study. For CIFAR10 with 40 labeled samples, $1.5K = 15$ reaches the best

Neighbor points(N)	$N=3$	$N=8$	$N=10$	$N=15$	$N=20$
Acc	82.71	94.21	95.04	95.55	95.21

Table 6: Ablation study with K neighbors on CIFAR10.

performance over the 5 choices. The result aligns with our intuition that fewer neighbors lack the information and too many neighbors may burden the LPA, for some may come from the other categories.

Conclusion

We first introduce **Theorem1** to prove that probability density helps to consider the *cluster assumption* comprehensively. Then, we introduce a probability-density-aware measurement, PM. We design a new algorithm with PM, the Probability-Density-Aware Label-Propagation algorithm(PMLP), that propagates pseudo-labels based on clusters’ geometric priors. **Theorem2** demonstrates PMLP’s exceptional performance, attributing it to integrating density information: LPA relying on traditional distance measurements is a particular case of PMLP. Extensive experiments are designed to show PMLP’s superiority.

Acknowledgements

The research is supported by the National Key R&D Program of China (Grant No. 2023YFA1008700 and 2023YFA1008703), the National Natural Science Foundation of China (NO. 62102151), the Open Research Fund of Key Laboratory of Advanced Theory and Application in Statistics and Data Science, Ministry of Education (KLATASDS2305), the Fundamental Research Funds for the Central Universities.

References

- Adam Coates, H. L., Andrew Ng. 2011. An analysis of single-layer networks in unsupervised feature learning. In *Proceedings of the fourteenth international conference on artificial intelligence and statistics*, pp. 215–223.
- Azizyan, M.; Singh, A.; and Wasserman, L. 2013. Density-sensitive semisupervised inference.
- Bengio, Y.; Lamblin, P.; Popovici, D.; and Larochelle, H. 2006. Greedy layer-wise training of deep networks. In *NeurIPS*.

- Berthelot, D.; Carlini, N.; Cubuk, E. D.; Kurakin, A.; Sohn, K.; Zhang, H.; and Raffel, C. 2019. Remixmatch: Semi-supervised learning with distribution alignment and augmentation anchoring.
- Bousquet, O.; Chapelle, O.; and Hein, M. 2003. Measure based regularization. In *NeurIPS*.
- Chapelle, O.; and Zien, A. 2005. Semi-supervised classification by low density separation. In *AISTATS*.
- Chen, H.; Tao, R.; Fan, Y.; Wang, Y.; Wang, J.; Schiele, B.; and Savvides, M. 2023. Softmatch: Addressing the quantity-quality trade-off in semi-supervised learning.
- Chen, T.; Kornblith, S.; Swersky, K.; Norouzi, M.; and Hinton, G. E. 2020a. Big self-supervised models are strong semi-supervised learners. In *NeurIPS*.
- Chen, X.; Chen, W.; Chen, T.; Yuan, Y.; Gong, C.; Chen, K.; and Wang, Z. 2020b. Self-pu: Self-boosted and calibrated positive-unlabeled training. In *ICML*.
- Douze, M.; Szlam, A.; Hariharan, B.; and Jégou, H. 2018. Low-shot learning with large-scale diffusion. In *CVPR*.
- Elezi, I.; Torcinovich, A.; Vascon, S.; and Pelillo, M. 2018. Transductive label augmentation for improved deep network learning. In *ICPR*.
- Guo, L. Z.; and Li, Y. F. 2022. Class-imbalanced semi-supervised learning with adaptive thresholding. In *ICML*.
- Hinton, G. E.; Osindero, S.; and Teh, Y. W. 2006. A fast learning algorithm for deep belief nets.
- Isen, A.; Toliás, G.; Avrithis, Y.; and Chum, O. 2019. Label propagation for deep semi-supervised learning. In *CVPR*.
- Krizhevsky, A.; and Hinton, G. 2009. Learning multiple layers of features from tiny images. Technical report.
- Laine, S.; and Aila, T. 2016. Temporal ensembling for semi-supervised learning.
- Lee, D. H. 2013. Pseudo-label: The simple and efficient semi-supervised learning method for deep neural networks. In *ICML*.
- Li, J.; et al. 2021. Comatch: Semi-supervised learning with contrastive graph regularization. In *ICCV*.
- Li, S.; Liu, B.; Chen, D.; Chu, Q.; Yuan, L.; and Yu, N. 2020. Density-aware graph for deep semi-supervised visual recognition. In *CVPR*.
- Miyato, T.; Maeda, S. I.; Koyama, M.; and Ishii, S. 2018. Virtual adversarial training: a regularization method for supervised and semi-supervised learning.
- Netzer, Y.; Wang, T.; Coates, A.; Bissacco, A.; Wu, B.; and Ng, A. Y. 2011. Reading digits in natural images with unsupervised feature learning. In *NeurIPS Workshop*.
- Nguyen, K. B. 2023. Boosting Semi-Supervised Learning by bridging high and low-confidence prediction. In *ICCV*.
- Nguyen, K. B. 2024. Debiasing, calibrating, and improving Semi-supervised Learning performance via simple Ensemble Projector. In *WACV*.
- Sajjadi, M.; Javanmardi, M.; and Tasdizen, T. 2016. Regularization with stochastic transformations and perturbations for deep semi-supervised learning. In *NeurIPS*.
- Shi, W.; Gong, Y.; Ding, C.; Tao, Z. M.; and Zheng, N. 2018. Transductive semi-supervised deep learning using min-max features. In *ECCV*.
- Sohn, K.; Berthelot, D.; Carlini, N.; Zhang, Z.; Zhang, H.; Raffel, C. A.; Cubuk, E. D.; Kurakin, A.; and Li, C. L. 2020. Fixmatch: Simplifying semi-supervised learning with consistency and confidence. In *NeurIPS*.
- Tarvainen, A.; and Valpola, H. 2017. Mean teachers are better role models: Weight-averaged consistency targets improve semi-supervised deep learning results. In *NeurIPS*.
- Vershynin, R. 2018. High-dimensional probability: An introduction with applications in data science. In *Vol. 47. Cambridge university press*.
- Wang, Y.; Chen, H.; Heng, Q.; Hou, W.; Fan, Y.; Wu, Z.; et al. 2022. Freematch: Self-adaptive thresholding for semi-supervised learning.
- Xu, N.; Zhang, X.; Wang, W.; Wang, J.; Guo, M.; and Cai, D. 2022. One positive label is sufficient: Single-positive multi-label learning with label enhancement. In *NeurIPS*.
- Yang, L.; Zhao, Z.; Qi, L.; Qiao, Y.; Shi, Y.; and Zhao, H. 2023. Shrinking class space for enhanced certainty in semi-supervised learning. In *ICCV*.
- Zhao, Z.; Zhou, L.; Wang, L.; Shi, Y.; and Gao, Y. 2022. LASSL: Label-guided self-training for semi-supervised learning. In *AAAI*.
- Zheng, M.; You, S.; Huang, L.; Wang, F.; Qian, C.; and Xu, C. 2022. Simmatch: Semi-supervised learning with similarity matching. In *CVPR*.
- Zhou, D.; Bousquet, O.; Lal, T.; Weston, J.; and Schölkopf, B. 2003. Learning with local and global consistency. In *NeurIPS*.

Appendix

Proof: Theorem1

Definition1.⁶ A zero-mean random variable X that satisfies

$$P(|X| \geq t) \leq 2 \exp(-t^2/K^2)$$

with any $t > 0, K \in R$ is called a sub-gaussian random variable. The sub-gaussian norm of X , denoted as $\|X\|_{\psi_2}$, is defined as: with any $t > 0$,

$$\|X\|_{\psi_2} = \inf\{t \geq 0 : \exp(X^2/t^2) \leq 2\}.$$

Definition2.⁷ A random vector X in R^d is called sub-gaussian vector if the one-dimensional marginals $\langle X, x \rangle$ are sub-gaussian random variables for all $x \in R^d$. The sub-gaussian norm of X is defined as:

$$\|X\|_{\psi_2} = \sup_{x \in S^{d-1}} \|\langle X, x \rangle\|_{\psi_2}.$$

S^{d-1} is the unit sphere with $d - 1$ dimension.

Lemma1. Without loss of generality, assume $X \in R^d$ is a sub-gaussian random vector with mean μ and $\|X\|_{\psi_2} \leq K$. Then for $t \in R^+$, with a constant C, c , there is:

$$P\{\|X\|_2 \geq CK\sqrt{d} + t\} \leq \exp(-\frac{ct^2}{K^2}),$$

Proof:

Without loss of generality (w.l.o.g), suppose X' is zero-mean gaussian random vector with $\|X'\|_{\psi_2} \leq K$. By **6.3.5** (Vershynin 2018), we have:

$$P\{\|BX'\|_2 \geq CK\|B\|_F + t\} \leq \exp(-\frac{ct^2}{K^2\|B\|_F^2}),$$

where $B \in R^{m \times d}$, $\|\cdot\|_F$ is the Frobenius norm, $\|\cdot\|_2$ represents the maximum of singular value.

Specifically suppose $B = I$, where $I \in R^{d \times d}$ is the identity matrix, there is:

$$P\{\|X'\|_2 \geq CK\sqrt{d} + t\} \leq \exp(-\frac{ct^2}{K^2}),$$

Change the zero-mean random vector X' to $X - \mu$ and complete the proof.

Lemma2. Assume two independent sub-gaussian random vectors $X_1, X_2 \in R^d$ with $\|X_1\|_{\psi_2} \leq K_1, \|X_2\|_{\psi_2} \leq K_2$ and corresponding constants C_1, C_2, c_1, c_2 , means μ_1, μ_2 . Denote $x_1 \in X_1, x_2 \in X_2$ are sampled from X_1, X_2 . Suppose $\gamma(x_1, x_2)$ is a continuous finite curve from x_1 to x_2 . Denote set of $\gamma(x_1, x_2)$ as $\Gamma(x_1, x_2)$. Define set A :

$$A = \{x : \|x - \mu_1\|_2 \geq C_1K_1\sqrt{d} + t_1\},$$

define set B :

$$B = \{x : \|x - \mu_2\|_2 \geq C_2K_2\sqrt{d} + t_2\},$$

⁶Vershynin, R. 2018. High-dimensional probability: An introduction with applications in data science. In Vol. 47. Cambridge university press.

⁷Vershynin, R. 2018. High-dimensional probability: An introduction with applications in data science. In Vol. 47. Cambridge university press.

with $t_1, t_2 \in R^+$. Assume X_1, X_2 sufficiently disperse with each other, satisfy:

$$\|\mu_1 - \mu_2\|_2 > C_1K_1\sqrt{d} + C_2K_2\sqrt{d} + t_1 + t_2.$$

Then with probability $(1 - \exp(-\frac{c_1t_1^2}{K_1^2}))(1 - \exp(-\frac{c_2t_2^2}{K_2^2}))$, we have the fact:

$$(A \cap B) \cap \gamma(x_1, x_2) \neq \emptyset.$$

Proof:

We first prove $A^c \cap B^c = \emptyset$: if there exist $x' \in A^c \cap B^c$, with triangle inequality, we have:

$$\|\mu_1 - \mu_2\|_2 \leq \|x' - \mu_2\|_2 + \|x' - \mu_1\|_2,$$

$$\|x' - \mu_2\|_2 + \|x' - \mu_1\|_2 \leq C_1K_1\sqrt{d} + C_2K_2\sqrt{d} + t_1 + t_2,$$

which contradicts our assumption.

Suppose $x_1 \in A^c, x_2 \in B^c$. As $\gamma(x_1, x_2)$ is a continuous finite curve from x_1 to x_2 , there exists $x' \in \gamma(x_1, x_2)$ satisfies:

$$\{x' \in \gamma(x_1, x_2), x' \in A \cap B\}.$$

Then we have:

$$\{x' : \|x' - \mu_1\|_2 \geq C_1K_1\sqrt{d}, \|x' - \mu_2\|_2 \geq C_2K_2\sqrt{d}\}.$$

With the assumption $x_1 \in A^c, x_2 \in B^c$, we conclude:

$$\{(A \cap B) \cap \gamma(x_1, x_2) \neq \emptyset\} = \{x_1 \in A^c, x_2 \in B^c\}.$$

With **Lemma1**, we have:

$$P(\{x_1 \in A^c, x_2 \in B^c\}) = P(\{x_1 \in A^c, x_2 \in B^c\} \neq \emptyset).$$

$$P(\{x_1 \in A^c, x_2 \in B^c\} \neq \emptyset) \geq (1 - \exp(-\frac{c_1t_1^2}{K_1^2}))(1 - \exp(-\frac{c_2t_2^2}{K_2^2})).$$

Complete the proof.

Lemma3. Set A, B are sets defined with parameter t_1, t_2 as **Lemma2**. Suppose we sample N_1 points from X_1 and N_2 points from X_2 . Take $t_1 < t_3 \in R, t_2 < t_4 \in R$ which satisfies:

$$K(\frac{\|t_3 - t_1\|_2^2}{h}) < \tau, K(\frac{\|t_4 - t_2\|_2^2}{h}) < \tau$$

with an exponential density kernel $K(\cdot)$, bandwidth h and threshold τ . Assume X_1, X_2 sufficiently disperse with each other:

$$\|\mu_1 - \mu_2\|_2 > C_1K_1\sqrt{d} + C_2K_2\sqrt{d} + t_3 + t_4.$$

Then, define set A', B' with t_3, t_4 as **Lemma2**. For any $x \in A' \cap B'$, calculate the probability density $p(x)$ with KDE. With $N_1 = N_2 \rightarrow \infty$, we conclude:

$$p(x) < \tau(1 - \frac{1}{2}(a_1 + a_2)) + \frac{1}{2}(a_1 + a_2),$$

and $\{\gamma(x_1, x_2) \cap x \in A' \cap B'\} \neq \emptyset$ with probability $(1 - a_3)(1 - a_4)$.

Here we simplify $a_1, a_3 = \exp(-\frac{c_1t_1^2}{K_1^2}), \exp(-\frac{c_1t_3^2}{K_1^2});$
 $a_2, a_4 = \exp(-\frac{c_2t_2^2}{K_2^2}), \exp(-\frac{c_2t_4^2}{K_2^2}).$

Proof:

Easy to prove that sub-gaussian vectors X_1, X_2 satisfies

$$E(|X_i|) < \infty, \quad i = 1, 2.$$

Thus X_1, X_2 satisfy the Law of Large Numbers. Suppose $N_1, N_2 \rightarrow \infty$, denote $N(A)$ as the number of elements in set A , we have:

$$\frac{N(A)}{N_1} = \exp(-\frac{c_1 t_1^2}{K_1^2}), \quad \frac{N(B)}{N_2} = \exp(-\frac{c_2 t_2^2}{K_2^2}).$$

With our assumption, for any $x \in A' \cap B'$, $x_i \in A^c \cup B^c$, we have:

$$\|x - x_i\|_2^2 \geq \min(\|t_3 - t_1\|_2^2, \|t_4 - t_2\|_2^2).$$

Then we have:

$$K\left(\frac{\|x - x_i\|_2^2}{h}\right) \leq K\left(\frac{\|t_3 - t_1\|_2^2}{h}\right) \leq \tau, \quad \text{or}$$

$$K\left(\frac{\|x - x_i\|_2^2}{h}\right) \leq K\left(\frac{\|t_4 - t_2\|_2^2}{h}\right) \leq \tau.$$

For $x \in (A' \cap B')$, with $N_1, N_2 \rightarrow \infty$, calculate $p(x)$ with KDE:

$$\begin{aligned} p(x) &= \frac{1}{N_1 + N_2} \sum_{i=1}^{N_1+N_2} K\left(\frac{\|x - x_i\|_2^2}{h}\right) \\ &\leq \frac{\sum_{(x_i \in A^c \cup B^c)} K\left(\frac{\|x - x_i\|_2^2}{h}\right)}{N_1 + N_2} + \frac{\sum_{(x_i \in A \cap B)} K\left(\frac{\|x - x_i\|_2^2}{h}\right)}{N_1 + N_2} \\ &\leq \tau P(A^c \cup B^c) + P(A \cap B) \\ &\leq \tau(1 - \frac{1}{2}(a_1 + a_2)) + \frac{1}{2}(a_1 + a_2), \end{aligned}$$

here we simplify $\exp(-\frac{c_i t_i^2}{K_i^2})$ as a_i , $i = 1, 2$.

A similar proof as in **Lemma2**, we have:

$$\{(A' \cap B') \cap \gamma(x_1, x_2) \neq \emptyset\} = \{x_1 \in (A')^c, x_2 \in (B')^c\}.$$

With the conclusion of **Lemma2**, we have:

$$P((A' \cap B') \cap \gamma(x_1, x_2) \neq \emptyset) \geq (1 - a_3)(1 - a_4).$$

Here we simplify a_3, a_4 as in the definition. Then complete the proof.

Theorem1 Suppose two sub-gaussian random vectors X_1, X_2 with mean μ_1, μ_2 . Denote x_1, x_2 randomly sampled from X_1, X_2 , and $\gamma(x_1, x_2)$ is a continuous finite path from x_1 to x_2 . For any $\tau \in R$. Denote $p(x)$ is the probability density of point x calculated with KDE, define event:

$$C_\tau : \{\exists x \in \gamma(x_1, x_2), p(x) \leq \tau\}.$$

Then with $\|\mu_1 - \mu_2\|_2^2 \rightarrow \infty$, we have:

$$P(C_\tau) \rightarrow 1.$$

Proof: From **Lemma3**, we have known with probability:

$$(1 - \exp(-\frac{c_3 t_1^2}{K_1^2}))(1 - \exp(-\frac{c_4 t_2^2}{K_2^2})),$$

there $\exists x \in \gamma(x_1, x_2)$, its probability density $p(x)$ from KDE satisfies:

$$p(x) \leq \tau(1 - \frac{1}{2}(a_1 + a_2)) + \frac{1}{2}(a_1 + a_2),$$

where $a_i = \exp(-\frac{c_i t_i^2}{K_i^2})$, $i = 1, 2$. Considering that t_3, t_4 satisfies:

$$\|\mu_1 - \mu_2\|_2 > C_1 K_1 \sqrt{d} + C_2 K_2 \sqrt{d} + t_3 + t_4,$$

when $\|\mu_1 - \mu_2\|_2 \rightarrow \infty$, we can take $t_3, t_4 \rightarrow \infty$. Considering t_1, t_2 satisfies:

$$K\left(\frac{\|t_3 - t_1\|_2^2}{h}\right) < \tau, \quad K\left(\frac{\|t_4 - t_2\|_2^2}{h}\right) < \tau,$$

easy to prove that we can take $t_1, t_2 \rightarrow \infty$. Then we have:

$$\lim_{t_3, t_4 \rightarrow \infty} (1 - \exp(-\frac{c_3 t_1^2}{K_1^2}))(1 - \exp(-\frac{c_4 t_2^2}{K_2^2})) \rightarrow 1,$$

$a_i = \lim_{t_i \rightarrow \infty} \exp(-\frac{c_i t_i^2}{K_i^2}) \rightarrow 0$, $i = 1, 2$.

Then we have the fact: when $\|\mu_1 - \mu_2\|_2 \rightarrow \infty$, with probability 1, we have the fact:

$$\{\exists x \in \gamma(x_1, x_2), \text{ satisfies } p(x) \leq \tau\}.$$

Then complete the proof.

Proof: Corollary1

Corollary1 Specifically take $\gamma(x_1, x_2)$ in **Theorem1** as a straight line and $x \in \gamma(x_1, x_2)$ distributes uniformly. For $\forall \tau \in R$, with sufficient large $\|\mu_1 - \mu_2\|_2^2$, we have:

$$\lim_{\|\mu_1 - \mu_2\|_2 \rightarrow \infty} P(\{x : p(x) \leq \tau, x \in \gamma(x_1, x_2)\}) \rightarrow 1.$$

Proof:

W.l.o.g, take $\forall M < 0.5$, take $|\mu_i| \rightarrow \infty, i = 1, 2$ and $\|\mu_1 - \mu_2\|_2 \rightarrow \infty$. Specifically take $|t_i| = M|\mu_i|, i = 1, 2$. It can be easily proved that we can further choose proper t_3, t_4 , so that $t_i, i = 1, 2, 3, 4$ satisfies the assumptions in **Lemma2** and **Lemma3**:

$$\|\mu_1 - \mu_2\|_2 > C_1 K_1 \sqrt{d} + C_2 K_2 \sqrt{d} + t_1 + t_2,$$

$$\|\mu_1 - \mu_2\|_2 > C_1 K_1 \sqrt{d} + C_2 K_2 \sqrt{d} + t_3 + t_4.$$

We denote the above assumptions with M as Ω_M . Then for x_i sampled from X_i , with **Lemma1**, we have:

$$P(x_i : \lim_{\|\mu_1 - \mu_2\|_2 \rightarrow \infty} \|x_i - \mu_i\|_2 \leq C_i K_i \sqrt{d} + t_i) \rightarrow 1.$$

Then as the setting in **Lemma2** and **Lemma3**, define A, B, A', B' with corresponding t_1, t_2, t_3, t_4 . Denote $l'(x_1, x_2), l''(x_1, x_2)$:

$$l'(x_1, x_2) = \{x \in \gamma(x_1, x_2), x \in A \cup B\},$$

$$l''(x_1, x_2) = \{x \in \gamma(x_1, x_2), x \in A' \cup B'\}.$$

Then with our assumption Ω_M we have:

$$\begin{aligned} \frac{\|l'(x_1, x_2)\|_2}{\|\gamma(x_1, x_2)\|_2} &\leq \frac{(1 - 2M)\|\mu_1 - \mu_2\|_2}{(1 + 2M)\|\mu_1 - \mu_2\|_2}, \\ \frac{(1 - 2M)\|\mu_1 - \mu_2\|_2}{(1 + 2M)\|\mu_1 - \mu_2\|_2} &\rightarrow \frac{1 - 2M}{1 + 2M} \end{aligned}$$

with probability 1.

With Ω_M , from **Lemma3**, it can be calculated that $\|t_i - t_j\|_2^2 \leq c(\tau)$, where $\{i = 1, j = 3\}$ or $\{i = 2, j = 4\}$,

$c(\tau) \in R$ is a constant with respect to τ, h and $K(\cdot)$. Then we have:

$$\lim_{t_1, t_2 \rightarrow \infty} \frac{\|l''(x_1, x_2)\|_2}{\|l'(x_1, x_2)\|_2} \rightarrow 1.$$

Then we have:

$$\lim_{t_1, t_2 \rightarrow \infty} \frac{\|l''(x_1, x_2)\|_2}{\|l(x_1, x_2)\|_2} \rightarrow \frac{1 - 2M}{1 + 2M},$$

for $\forall M \leq 0.5$.

W.l.o.g, take $M \rightarrow 0$, we have:

$$\lim_{t_1, t_2 \rightarrow \infty} \frac{\|l''(x_1, x_2)\|_2}{\|l(x_1, x_2)\|_2} \rightarrow \frac{1 - 2M}{1 + 2M} = 1,$$

Considering $x \in \gamma(x_1, x_2) = l(x_1, x_2)$ is uniformly distributed, we have:

$$\lim_{\|\mu_1 - \mu_2\|_2^2 \rightarrow \infty} \frac{P(x \in \gamma(x_1, x_2))}{P(x \in \gamma'(x_1, x_2))} \rightarrow 1.$$

With **lemma3** and **Theorem1**, we have the fact: the event, $\{x \in \gamma(x_1, x_2), p(x) \leq \tau\}$, holds with probability 1.

Complete the proof.

Proof: Theorem2

Lemma4. Suppose pseudo-label \hat{Y}^{LP} is propagated with an affinity matrix W , and \hat{Y}'^{LP} is propagated by an affinity matrix W' :

$$\begin{aligned} \hat{Y}^{LP} &= (I - \alpha D^{-\frac{1}{2}} W D^{-\frac{1}{2}})^{-1} Y^{LP, \text{high}}, \\ \hat{Y}'^{LP} &= (I - \alpha D'^{-\frac{1}{2}} W' D'^{-\frac{1}{2}})^{-1} Y^{LP, \text{high}}. \end{aligned}$$

Moreover, suppose $W = kW', k \in R$, and D and D' are two diagonal matrices with their (i, i) -th elements being the sum of the i -th row of W and W' respectively. Then we have

$$\hat{Y}'^{LP} = \hat{Y}^{LP}$$

Proof:

$$\begin{aligned} \hat{Y}'^{LP} &= (I - \alpha D'^{-\frac{1}{2}} W' D'^{-\frac{1}{2}})^{-1} Y^{LP, \text{high}} \\ &= (I - \alpha (kD)^{-\frac{1}{2}} (kW) (kD)^{-\frac{1}{2}})^{-1} Y^{LP, \text{high}} \\ &= (I - \alpha (\frac{1}{\sqrt{k}} D^{-\frac{1}{2}}) (kW) (\frac{1}{\sqrt{k}} D^{-\frac{1}{2}}))^{-1} Y^{LP, \text{high}} \\ &= (I - \alpha D^{-\frac{1}{2}} W D^{-\frac{1}{2}})^{-1} Y^{LP, \text{high}} \\ &= \hat{Y}^{LP} \end{aligned}$$

The proof is completed.

Theorem2. Denote the model parameter in one iteration as θ . And let \mathcal{L}_U be the unsupervised loss between predictions and pseudo-labels. Denote Y^P as the set of predictions, \hat{Y}^{*LP} and \hat{Y}^{LP} be the pseudo-labels generated by PMLP and traditional LPA with any $D(\cdot, \cdot)$. Suppose we calculate the probability density by KDE with exponential kernel and bandwidth h . Then \mathcal{L}_U satisfies:

$$\min_{\theta \in \Theta, h \in R} \mathcal{L}_U(Y^P, \hat{Y}^{*LP}) \leq \min_{\theta \in \Theta} \mathcal{L}_U(Y^P, \hat{Y}^{LP}).$$

Proof: To prove **Theorem2**, it suffices to prove that:

$$\min_{\theta \in \Theta} \mathcal{L}_U(Y^P, \hat{Y}^{LP}) = \min_{\theta \in \Theta, h=h^*} \mathcal{L}_U(Y^P, \hat{Y}^{*LP}).$$

Then there is:

$$\begin{aligned} \min_{\theta \in \Theta, h \in R} \mathcal{L}_U(Y^P, \hat{Y}^{*LP}) &\leq \min_{\theta \in \Theta, h=h^*} \mathcal{L}_U(Y^P, \hat{Y}^{*LP}), \\ \min_{\theta \in \Theta, h=h^*} \mathcal{L}_U(Y^P, \hat{Y}^{*LP}) &= \min_{\theta \in \Theta} \mathcal{L}_U(Y^P, \hat{Y}^{LP}), \end{aligned}$$

which can complete the proof.

Denote \hat{Y}^{*LP} with $h = h^*$ as $\hat{Y}^{*LP}(h^*)$, it suffices to prove that $\hat{Y}^{*LP}(h^*) = \hat{Y}^{LP}$.

Denote the set of high-confidence predictions as $Y^{LP, \text{high}}$, the set of low-confidence predictions as $Y^{LP, \text{low}}$, the affinity matrix W , with hyper-parameter α, η in pseudo-labeling. Then there is:

$$\hat{Y}^{LP} = \eta(I - \alpha D^{-\frac{1}{2}} W D^{-\frac{1}{2}})^{-1} Y^{LP, \text{high}} + (1 - \eta) Y^{LP, \text{low}},$$

note that PMLP's affinity matrix W' is adjusted by density information $I(p_{i,j})$ corresponding to bandwidth h , then there is:

$$\hat{Y}^{*LP}(h) = \eta(I - \alpha D'(h)^{-\frac{1}{2}} W'(h) D'(h)^{-\frac{1}{2}})^{-1} Y^{LP, \text{high}} + (1 - \eta) Y^{LP, \text{low}}.$$

Then to prove $\hat{Y}^{*LP}(h^*) = \hat{Y}^{LP}$, it suffices to show that

$$D'(h^*)^{-\frac{1}{2}} W'(h^*) D'(h^*)^{-\frac{1}{2}} = D^{-\frac{1}{2}} W D^{-\frac{1}{2}}, \quad \text{with } h^* \in R.$$

Denote that

$$W_{i,j} = \begin{cases} 0, & \text{if } i = j, \\ D(o_i^{LP}, o_j^{LP}), & \text{if } i \neq j, \end{cases}$$

$$W'_{i,j}(h) = \begin{cases} 0, & \text{if } i = j, \\ I(p_{i,j}(h)) D(o_i^{LP}, o_j^{LP}), & \text{if } i \neq j. \end{cases}$$

Denote $p_{i,j}^l(h)$, $l \in \{1, 2, \dots, k\}$ represents the density of the point $o_{i,j}^l$, $l \in \{1, 2, \dots, k\}$, where $o_{i,j}^l$ represents the l -th-equal division points between two features $o_i^{LP}, o_j^{LP} \in O^{LP}$. To calculate the density $\{p_{i,j}^1, \dots, p_{i,j}^k\}$, for each point $o_{i,j}^l$, we select n points in its neighbor: $\{o_{i,j}^{l,1}, \dots, o_{i,j}^{l,n}\}$, and calculate $p_{i,j}^l$ with KDE whose bandwidth is set as h :

$$p_{i,j}^l(h) = \frac{1}{nh} \sum_{m=1}^n K\left(\frac{\|o_{i,j}^{l,m} - o_{i,j}^l\|_2}{h}\right),$$

Without loss of generality, we take $I(p_{i,j})$ as the average k equal division points' density as $p_{i,j}$:

$$p_{i,j}(h) = \frac{1}{nhk} \sum_{l=1}^k \sum_{m=1}^n K\left(\frac{\|o_{i,j}^{l,m} - o_{i,j}^l\|_2}{h}\right),$$

where $K(\cdot)$ is a Exponential kernel satisfies:

$$K(x) = \exp(-x).$$

With **Lemma3**, it equals to update W with:

$$W'_{i,j}(h) = \begin{cases} 0, & \text{if } i = j, \\ p'_{i,j}(h) D(o_i^{LP}, o_j^{LP}). & \text{if } i \neq j, \end{cases}$$

to get a same $\widehat{Y}^{*LP}(h)$, where $p'_{i,j}$ satisfies:

$$p'_{i,j}(h) = \frac{1}{nk} \sum_{l=1}^k \sum_{m=1}^n K\left(\frac{o_{i,j}^{l,m} - o_{i,j}^l}{h}\right),$$

When $h \rightarrow \infty$, there is:

$$\lim_{h \rightarrow \infty} p'_{i,j}(h) = \lim_{h \rightarrow \infty} \frac{1}{nk} \sum_{l=1}^k \sum_{m=1}^n K\left(\frac{o_{i,j}^{l,m} - o_{i,j}^l}{h}\right) = 1.$$

Then we have

$$\lim_{h \rightarrow \infty} p'_{i,j}(h) = 1, \quad \lim_{h \rightarrow \infty} W'(h) = W.$$

That is denote $h^* = \infty$, there is:

$$\widehat{Y}^{*LP}(h^*) = \widehat{Y}^{LP},$$

$$\min_{\theta \in \Theta, h \in R} L_U(Y^{LP}, \widehat{Y}^{*LP}) \leq \min_{\theta \in \Theta, h^* = \infty} L_U(Y^{LP}, \widehat{Y}^{*LP}(h^*)),$$

$$L_U(Y^{LP}, \widehat{Y}^{*LP}(h^*)) = \min_{\theta \in \Theta} L_U(Y^{LP}, \widehat{Y}^{LP}).$$

Complete the proof. The case when $I(p_{i,j})$ takes maximum, minimum or t-quantile between $\{p(x_{i,j}^1, \dots, p(x_{i,j}^k))\}$ can be proved in a similarity way.

PMLP Generates Better Pseudo-labels: Extension

We demonstrate that PMLP can generate more accurate pseudo-labels in the main context. This section presents additional examples with different datasets to prove that PMLP can generally produce more correct pseudo-labels. It can be seen from Fig. 4 and Fig. 5 that with a more considerable amount of labeled data, PMLP still performs better than LPA and can generate more accurate pseudo-labels.

GPU Based KDE: Details

The KDE from Sklearn runs only on the CPU, which slows down PMLP's calculation. To accelerate PMLP, we design the GPU-based KDE: Given the chosen point $o_{i,j}$ and the neighboring points $o_{i,j}^1, \dots, o_{i,j}^n$, we calculate $p_{i,j}(h)$ on the GPU as follows:

$$p_{i,j}(h) = \frac{1}{n} \sum_{m=1}^n K\left(\frac{\|o_{i,j}^{l,m} - o_{i,j}^l\|_2}{h}\right).$$

In our approach, we renew a GPU-based KDE algorithm, which can be seen in the algorithm 2. The algorithm can accelerate the KDE significantly, as seen in the main context's experiments.

Toward Better $I(p_{i,j})$: Extension

We have studied which choice of $I(p_{i,j})$ is better in the main context by comparing the performance of PMLP with different $I(p_{i,j})$ on CIFAR10, 40 labeled samples. The result suggests that $avg\{p_t(i,j), t = 1, 2, \dots, k\}$ and $Q_t\{p_t(i,j), t = 1, 2, \dots, k\}$ tend to have a stable good performance and $max\{p_t(i,j), t = 1, 2, \dots, k\}$ or $min\{p_t(i,j), t = 1, 2, \dots, k\}$ is unstable.

In this section, we show the unstable of $max\{p_t(i,j), t = 1, 2, \dots, k\}$ or $min\{p_t(i,j), t = 1, 2, \dots, k\}$ dues to their sensitivity to neighbor's densities. We first define density ratio

Algorithm 2: Quick density-aware approach

Input: the set of features O^{LP} , τ , k , the set of midpoints $\{\frac{o_i^{LP} + o_j^{LP}}{2}\}$, $i, j \in \{1, \dots, k\}$, the n neighbor points for different midpoints, $\{o_{i,j}^1, \dots, o_{i,j}^n\}$, $i, j \in \{1, \dots, k\}$, Exponential kernel $K(\cdot)$, bandwidth h .

Output: updated threshold $p_{i,j}$.

- 1: Divide the set of features O^{LP} into $O^{LP,high}$, $O^{LP,low}$ by threshold τ ;
 - 2: For any $o_i^{LP} \in O^{LP,low}$, select the k nearest neighbor points in $O^{LP,high}$ and calculate the midpoints $\{\frac{o_i^{LP} + o_j^{LP}}{2}\}$, $i, j \in \{1, \dots, k\}$;
 - 3: Choose the n nearest neighbor points for each $\frac{o_i^{LP} + o_j^{LP}}{2}$, get $\{o_{i,j}^1, \dots, o_{i,j}^n\}$, $i, j \in \{1, \dots, k\}$;
 - 4: **for each** $o_{i,j}^m$, **do**
 - 5: Calculate $K(\frac{\|o_{i,j}^{l,m} - o_{i,j}^l\|_2}{h})$;
 - 6: **end for**
 - 7: Average the n $K(\frac{\|o_{i,j}^{l,m} - o_{i,j}^l\|_2}{h})$ with $\frac{1}{n}$, without h .
-

Bandwidth	h=5	h=10	h=100	LASSL
$max\{p_t(i,j)\}$	92.72± 3.38	95.29± 0.86	95.06±0.61	95.07±0.78
R_h , density-ratio	1.3	1.15	1.01	1
$min\{p_t(i,j)\}$	92.42± 2.3	95.13± 0.81	95.03±0.64	95.07±0.78
R_h , density-ratio	1.3	1.15	1.01	1

Table 7: Ablation study on CIFAR10 with 40 labeled data. We modify bandwidth h to diminish the influence of density information $max\{p_t(i,j)\}$ and $min\{p_t(i,j)\}$. It can be seen $max\{p_t(i,j)\}$ and $min\{p_t(i,j)\}$ are sensitive to density information and comparably unstable compared to $avg\{p_t(i,j)\}$.

$R_h = \frac{max\{p_t(i,j), t=1,2,\dots,k\}}{min\{p_t(i,j), t=1,2,\dots,k\}}$ and estimate R_h by randomly sampling 1000 pairs of $p_t(i,j)$ from the former 5 epoches. As discussed in the main text, $I(p_{i,j})$ is not a sufficient statistic for reflecting the *cluster assumption* and R_h can reflect our confidence in detecting the *cluster assumption* with $max\{p_t(i,j), t = 1, 2, \dots, k\}$ and $min\{p_t(i,j), t = 1, 2, \dots, k\}$.

In the main context, we choose the bandwidth $h = 5$, with $R_h = 1.3$. When the bandwidth increases to $h = 10, 100$, the density ratio decreases to 1.15, 1.01 and restrains the influence of singular points. We deploy our experiments on the CIFAR10 dataset with 40 labeled samples, choose $k = 3$, and repeat the experiments thrice. As can be seen in Tab. 7, with lower R_h , the $max\{p_t(i,j), t = 1, 2, \dots, k\}$ and $min\{p_t(i,j), t = 1, 2, \dots, k\}$ tend to get a stable good performance, which reveals that $max\{p_t(i,j), t = 1, 2, \dots, k\}$ and $min\{p_t(i,j), t = 1, 2, \dots, k\}$ are sensitive to point's density and thus can be easily affected by singular values. A large bandwidth h helps reduce R_h and can help get a stable result.

It seems that decreasing R_h can help to stabilize the

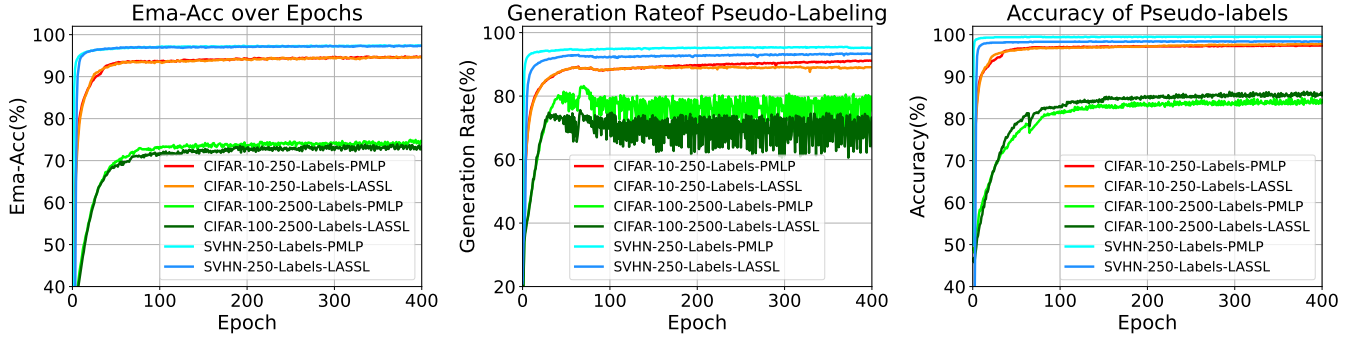


Figure 4: The accuracy, rate of high-quality predictions, and accuracy of pseudo-labels on CIFAR10 with 250 labeled data, CIFAR100 with 2500 labeled data, and SVHN with 250 labeled data. It can be seen that PMLP can still produce more correct pseudo-labels, which conform to our conclusion in the main context.

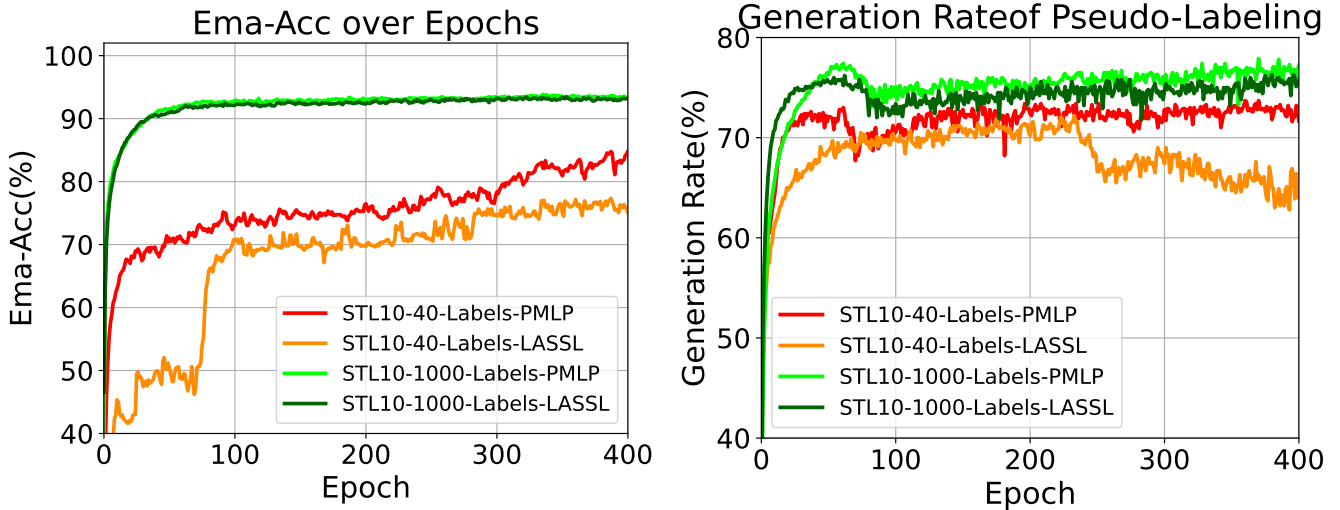


Figure 5: The accuracy and rate of high-quality predictions on STL-10 with 40 and 1000 labeled data. It can be seen that PMLP can still produce more correct pseudo-labels, which conform to our conclusion in the main context.

$\max\{p_t(i, j), t = 1, 2, \dots, k\}$ and $\min\{p_t(i, j), t = 1, 2, \dots, k\}$. However, by **theorem2**, $\lim_{h \rightarrow \infty} R_h \rightarrow 1$, which means the cost is to diminish density information $I(p_{i,j})$ and degenerating PMLP to LPA. As seen in Tab. 7, when $h = 10$, $\max\{p_t(i, j), t = 1, 2, \dots, k\}$ and $\min\{p_t(i, j), t = 1, 2, \dots, k\}$ tend to be better. However, when $h = 10$, the standard deviation of $\max\{p_t(i, j), t = 1, 2, \dots, k\}$ and $\min\{p_t(i, j), t = 1, 2, \dots, k\}$ is **0.86** and **0.81**, which is larger than $\text{avg}\{p_t(i, j), t = 1, 2, \dots, k\}$'s **0.32** in the main context. To this issue, we conclude that $\text{avg}\{p_t(i, j), t = 1, 2, \dots, k\}$ is the better choice of $I(p_{i,j})$.

Ablation Study: Toward The Balance with Time and Accuracy

In PMLP, we specifically, here we take $I(P_{i,j})$ as $\text{avg}\{p_t(i, j), t = 1, 2, \dots, k\}$ or $Q_t\{p_t(i, j), t = 1, 2, \dots, k\}$, where $p_t(i, j)$ are chosen from the connecting line $l(x_1, x_2)$ with the equal distance. A natural thought goes that increasing k will improve PMLP's robustness: view $I(p_{i,j})$ as a

random variable, more samples help to get a stable and accurate result due to the law of large numbers. However, increasing K will increase the time for KDE. In this section, we compare the time consumption of different k . We deploy PMLP with $K = 1, 3, 5$ on CIFAR10 with 40 labeled data, and the $I(p_{i,j})$ is chosen as $\text{avg}\{p_t(i, j), t = 1, 2, \dots, k\}$. It can be seen in Tab. 8 that with k increase, the time consumption increases obviously. From our main context, PMLP with $K = 1$ only increases about 3% time consumption compared with baseline LASSL, but when $K = 3$, the PMLP increases about 18% time consumption compared with our baseline LASSL. When $k = 5$, the PMLP increases about 47% time consumption compared with our baseline LASSL. As the main context shows, $k = 3, 5$ can not bring an apparent breakthrough, and $k = 1$ has significantly improved PMLP than traditional LPA. This motivates us to believe that choosing $k = 1$ is enough to achieve PMLP's superior performance without adding too much calculation burden.

Number of points	Overall Average Time (s/epoch)	Average Time Across Different Iterations (s/epoch)			
		1-256	257-512	513-768	769-1024
baseline, LASSL	211.41	255.52	196.10	196.66	197.35
PMLP, K=1	217.94	260.05	203.72	203.52	204.46
Relative Time Increase vs baseline	+3.1%	+1.75%	+3.9%	+3.49%	+3.6%
PMLP, K=3	248.82	285.31	236.08	236.65	237.23
Relative Time Increase vs K=1	+14.14%	+9.72%	+15.89%	+16.28%	+16.03%
Relative Time Increase vs baseline	+17.7%	+11.66%	+20.39%	+20.33%	+20.21%
PMLP, K=5	310.25	381.09	307.12	276.55	276.23
Relative Time Increase vs K=1	+42.48%	+46.54%	+50.76%	+35.88%	+35.10%
Relative Time Increase vs baseline	+46.75%	+49.14%	+56.61%	+40.62%	+39.97%

Table 8: Comparison of overall average time and average time across different training phases for different methods on STL-10 and CIFAR-10 datasets.

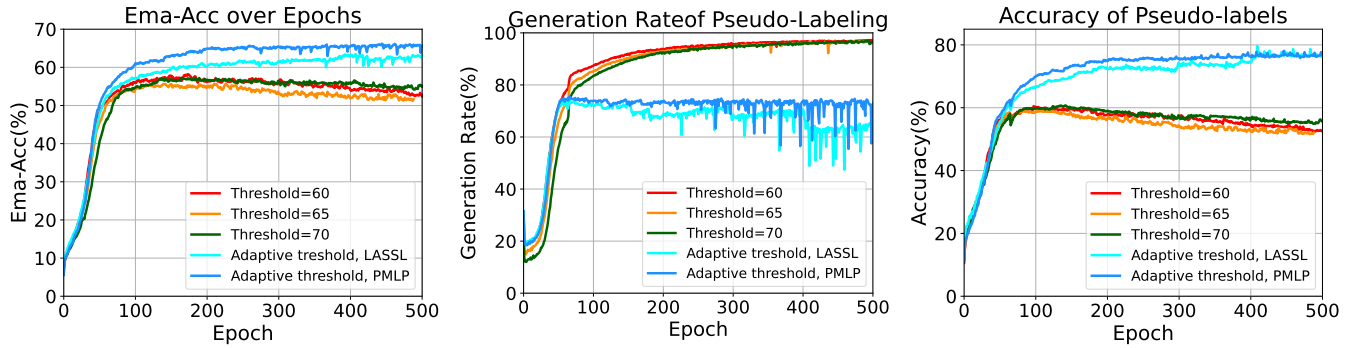


Figure 6: The accuracy, rate of high-quality predictions, and correct pseudo-label ratios. It can be seen that LASSL with tuning strategy outperforms the LASSL with fixed τ . With the same tuning strategy, PMLP outperforms the LASSL.

Algorithm 3: Adaptive threshold tuning strategy

Input: predictions Y^P , the threshold τ from the last iteration, counting number i , training epoch n . **Output:** updated threshold τ .

```

1: for  $n = 1$  to 1024 do
2:   for each iteration: do
3:     if  $p_{i,j} > \tau$  then
4:        $i=i+1$ ;
5:     end if
6:     if  $i > 50$  then
7:        $\tau = \tau + 10^{1+\lceil -\frac{n}{200} \rceil}$ ;
8:     end if
9:   end for
10: end for

```

An Adaptive Threshold Tuning Strategy

In the baseline model LASSL, high-confidence pseudo-labels are selected for training, defined as $y_i^{LP, \text{high}} = I(\max(y_i^{LP}) \geq \tau)y_i^{LP}$. The threshold for assigning a high-quality label is set to $\tau = 0.95$ across all experiments on SVHN, CIFAR10, and CIFAR100 datasets.

However, in our implementations, $\tau = 0.95$ does

not suit the experiments with CIFAR100. When $\tau \in \{0.6, 0.65, 0.7, 0.75, 0.8, 0.9, 0.95\}$, PMLP performs best with $\tau \in \{0.6, 0.65, 0.7\}$. Fig. 6 shows PMLP’s accuracy, the ratio of pseudo-labels exceeding τ , and the ratio of high-confidence pseudo-labels correct with the ground truth under different fixed τ values.

The high-confidence pseudo-labels will affect the model’s training by misleading the unsupervised loss L_U :

$$L_U = I(y_j^U \geq \tau)H(Y^U, Y^P),$$

where we encourage the prediction vector Y^P and pseudo-label Y^U to be consistent. From Fig. 6, when τ is high, few high-confidence predictions are accepted and help decrease L_U . Contrastingly, a fixed low threshold τ increases the number of high-confidence pseudo-labels, but nearly half are incorrect, which introduces harmful, wrong information. In a word, incorrect pseudo-labels due to a fixed threshold τ negatively impact PMLP’s training.

To improve PMLP’s performance, we introduce an adaptive threshold policy for τ , as shown in algorithm 3. In each training iteration, we define r :

$$r = \frac{1}{|Y^P|} \sum_{j=1}^{|Y^P|} I(y_j^U \geq \tau),$$

which reflects the ratio of high-quality predictions. PMLP generates pseudo-labels with the *cluster assumption*, and its consistency is encouraged by a consistency loss L_C ; a model is expected to create more high-quality predictions during its training. Thus, we can slightly increase the threshold τ to foster a more confident model. Fig. 6 also shows the superior performance of the adaptively tuning strategy. All comparative experiments are conducted on the same GPU. CIFAR10 experiments are performed on a GeForce RTX 3090, and CIFAR100 experiments are performed on a GeForce RTX 4090. The results show that PMLP does not significantly increase training time.